Adsorption of copper ions from solution using xanthate wheat straw

Qiehui Guo, Zhongyang Zang, Jie Ma, Jingyi Li, Tong Zhou and Runping Han

ABSTRACT

To enhance adsorption capacity of wheat straw (WS) toward copper ion from solution, carbon disulfide was used to modify WS by a facile grafting method through epichlorohydrin and ethylenediamine. So WS containing xanthate groups (XWS) was obtained. The XWS was characterized using elemental analysis, X-ray diffraction, infrared spectroscopy and adsorption property of XWS toward copper ions. The results showed that S was introduced into the surface of WS. The solution pH was in favor of Cu^{2+} adsorption at pH 5, while NaCl existing in solution was slightly favorable for adsorption. The adsorption kinetic followed the pseudo-second-order kinetic model, while the adsorption isotherm curve was well fitted using the Langmuir model. The adsorption capacity was 57.5 mg·g^{-1} from experiment. The process was entropy-produced, endothermic and spontaneous in nature. The column adsorption was performed and Yan model was good to predict the breakthrough curve. XWS as adsorbent is promising to remove copper ions from solution, and this offers one way of effective utilization of waste byproduct from agriculture.

Key words | adsorption, copper ion, modified wheat straw, thermodynamic analysis

Qiehui Guo
Zhongyang Zang
Jie Ma
Jingyi Li
Tong Zhou
Runping Han (corresponding author)
College of Chemistry,
Zhengzhou University,
No. 100 Kexue Road, Zhengzhou 450001,
China
E-mail: *rphan67@zzu.edu.cn*

HIGHLIGHTS

- Xanthate wheat straw was prepared and characterized.
- Adsorption capacity was significantly improved after modification.
- Adsorption performance was carried out in batch and column modes.
- The breakthrough curves in column mode can be fitted by Yan model.

doi: 10.2166/wst.2020.487

GRAPHICAL ABSTRACT

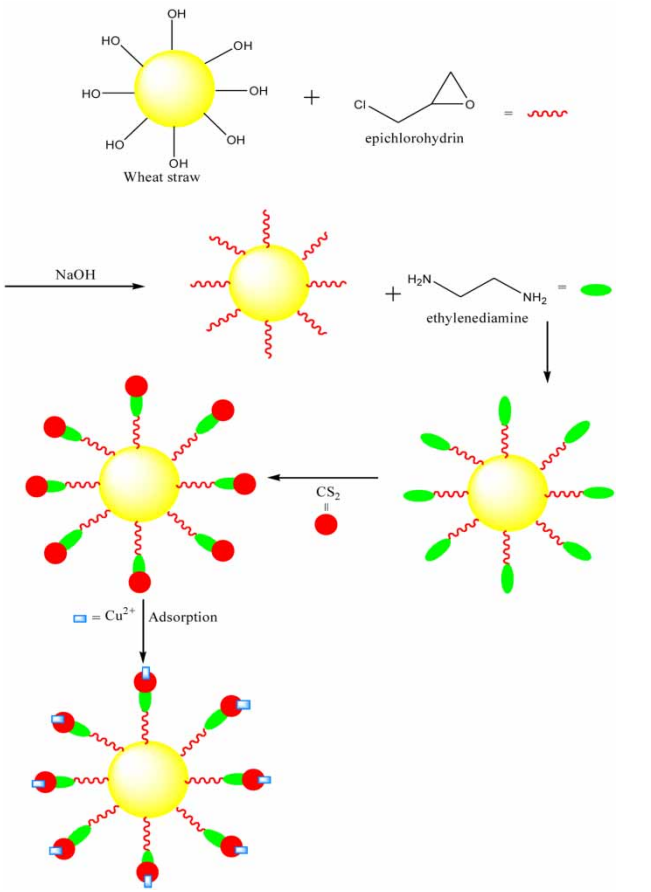

INTRODUCTION

With the rapid growth of the global population and the rapid development of modern industry, the human demand for water resources is increasing at an alarming rate, but at the same time, the pollution of water resources is becoming increasingly serious. Heavy metal pollution has become one of the most harmful water pollution problems in recent years (Fu & Wang 2011). Generally, heavy metals in environmental pollution refer to biological or toxic heavy metals such as mercury, cadmium, lead, chromium, zinc and copper. The heavy metal ions of pollutants come from the following industries: mining, electroplating, paper making, batteries, fertilizers, leather, pesticides, etc. (Yu *et al.* 2020). The water has a certain self-purification function. After a small amount of heavy metal ions enter the water body, the water body can be treated by itself without affecting the environment. However, with the development of industry, a large number of heavy metals enter the water body. Heavy metal ions are not biodegradable and can accumulate in organisms. Copper is an essential trace element in human body and an integral part of various enzymes. However, if copper ions exceed a certain threshold in the body, they will cause liver, kidney, capillary and central nervous system damage.

The removal methods of heavy metal ions in water mainly include precipitation, ion exchange, membrane filtration, photocatalytic degradation, oxidation, flocculation and adsorption (Fu & Wang 2011; Hashim *et al.* 2011). The adsorption method has many advantages, such as being suitable for the treatment of dilute solution, high enrichment multiple, good separation effect, high product quality, easy liquid-solid separation, no secondary pollution and emulsification, and adsorbents can be recycled, so it has become one

of the most widely applied and promising technologies (Zhou *et al.* 2019; Yu *et al.* 2020).

Compared with activated carbons, zeolites, fibers, organic resins and so on, adsorbents from a variety of agro-forestry wastes have been applied in wastewater treatment because of their advantages: easy to obtain, low cost, easy operations, and availability (Zhang *et al.* 2014).

At present, straw and many plant materials, such as banana leaves, potato skins, cocoa shells, rye straw, corn cobs, peach shells, discarded tea leaves, etc. are selected as adsorbents to remove pollutants from water (Bhatnagar & Sillanpaa 2010). Wheat straw (WS) is one by-product of agricultural production; there is the natural synthesis of large amounts every year. WS is often disposed of as waste, and this does not lead to effective use of this resource. So it is necessary to develop one way for full utilization of these materials. The main components of WS are cellulose, hemicellulose, lignin, etc., and it can be directly applied as adsorbent. Raw WS was used to treat aqueous solutions containing Cu^{2+}, Zn^{2+} and Ni^{2+} and the maximum adsorption capacities were 5 $mg{\cdot}g^{-1}$, 2.5 $mg{\cdot}g^{-1}$ and 3.25 $mg{\cdot}g^{-1}$, respectively (Gorgievski *et al.* 2013). Although straw has a certain adsorption capacity for pollutants, its adsorption capacity is relatively weak. In order to improve the adsorption property of WS, a simple chemical modification is needed. Amine group-modified agro-wastes have been studied a lot. Amino groups are used to enhance the adsorption properties of anionic dyes and metal ions (Xu *et al.* 2011; Shang *et al.* 2016; Dong *et al.* 2019; Li *et al.* 2020). Zhong *et al.* prepared amphoteric wheat stalks by reacting epoxy wheat stalks with ethylenediamine, triethylamine and chloroacetic acid, studied the adsorption of Cu(II) and Cr(VI) on modified wheat stalks, and fitted them with kinetic model and adsorption isothermal model (Zhong *et al.* 2014). Ethylenediamine and triethylamine, diethylenetriamine, dimethylamine, etc. are often considered to modify materials (Deng & Ting 2005). Disulfide carbon can react with amino groups in basic conditions and xanthate can be obtained. Xanthate can effectively bind some heavy metal ions, such as Cu^{2+}, Pb^{2+} and Hg^{2+}. So disulfide carbon modified materials can be prepared and the adsorbents with xanthate group can selectively remove metal ions (Chauhan & Sankaramakrishnan 2008; Liang *et al.* 2009). But there is no study about WS as adsorbent in this direction.

In this paper, xanthated wheat straw (XWS) was prepared with reaction between CS_2 and ethylenediamine grafted to surface of WS through epichlorohydrin. The adsorption property of Cu^{2+} by XWS was presented in batch mode, while breakthrough curve was also discussed. Copper ion is selected in this study as copper is widely used in various industries and has negative effects on environment and human beings when there is high level of copper ions in the effluent. Regeneration performance of the spent adsorbent was also explored.

MATERIALS AND METHODS

Instruments and reagents

The WS was obtained from Zhengzhou suburb. All of the chemical reagents used in this research, including epichlorohydrin (ECH), ethylenediamine (EDA), CS_2, Na_2SO_4, $CaCl_2$, NaCl, HCl, Cu $(NO_3)_2{\cdot}3H_2O$, NaOH and 95% ethanol, all of analytical purity, were supplied by Sinopharm Chemical Reagent Co., Ltd, China. The laboratory water was deionized water.

Stock solution of Cu^{2+} was prepared by dissolving $Cu(NO_3)_2{\cdot}3H_2O$ in deionized water, and the further working solution was obtained by daily dilution to a suitable concentration. Solution pH was adjusted using different concentrations of HCl and NaOH.

Instruments used in this research are the following: pH-mV meter (LeiCi PHS-3S, China), air bath shaker (GuoHua SHZ-82, China), UV spectrophotometer (Shimadzu brand UV-3000), X-ray diffraction (D/MAX-RA, Rigaku, Japan), Fourier infrared spectrometer (PE-1710FTIR, American PE Company), X-ray fluorometer (S4PIONEER, Germany, Brock Company), scanning electron microscope (JSM-6700F, Nippon Electronics), elemental analyzer (Flash EA 1112, Thermo Electron Corporation), peristaltic pump (BT100-2 J, Baoding Langge Constant Current Pump Co. Ltd), mill (JL-02A, Shanghai Jiarui Tools Co. Ltd).

Preparation of absorbent

The preparation of ethylenediamine modified WS (EDA-WS) was through grafting reaction using ECH (ECH modified WS, ECH-WS) followed previous work (Wang *et al.* 2011). Next step was to modify the EDA-WS with CS_2 via xanthan acidification reaction. Put the EDA-WS into a 500 mL conical flask, add 200 mL 1.0 $mol{\cdot}L^{-1}$ NaOH, 12 ml CS_2 and 40 mL 95% ethanol, and place the conical flask in a thermostatic oscillator to oscillate for 5 h at 313 K. The xanthan acidified straw (XWS) is filtered and washed with ethanol to remove the unreacted CS2. The modified straw is again washed with distilled water to neutral at 353 K before being dried at 60 °C in an oven.

The chemical reactions in the modification process are as follows:

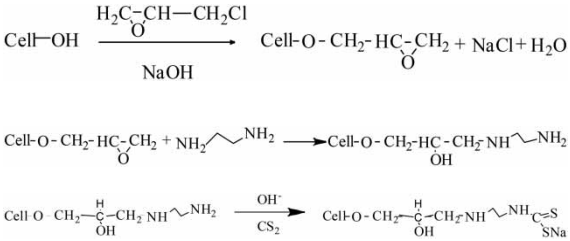

Characterization of materials

Several analytical techniques were used to characterize the adsorbents. The pH at point zero charge of WS and XWS was obtained by the 0.01 mol·L^{-1} NaCl solid addition method. Fourier transform infrared spectroscopy (FTIR Spectrometer, Nicolet iS50, USA) was used to confirm the characteristic functional groups of WS and XWS. The contents of nitrogen, carbon, hydrogen and sulfur elements were determined by automatic element analyzer (Flash EA 1122, Thermo Fisher Scientific). The crystal textures were imaged by X-ray powder diffractometer (D/MAX-RA, Japan).

Adsorption experiments in batch mode

The removal of Cu^{2+} from aqueous solution by XWS was studied on a Thermostatic shaker (SHZ-82) at constant speed (120 rpm) in batch mode. A certain amount of absorbent (10 mg) was placed in a 50 mL Erlenmeyer flask, into which was added 10 mL of Cu^{2+} of initial known concentration (50 mg·L^{-1} except adsorption isotherm study) with solution pH 5.0 (except effect of solution pH) at 303 K. After adsorption, mixtures were filtered and the residual Cu^{2+} concentration in filtrate was measured using atomic absorption spectrophotometry at wavelength of 324.7 nm (Perkin–Elmer, AAanalyst 300).

The adsorption capacity (q_t or q_e) of Cu^{2+} onto unit weight of XWS and removal percentage were calculated according to the following equations:

$$q = \frac{V(C_0 - C)}{m} \quad (1)$$

where C_0 is the initial Cu^{2+} concentration (mg·L^{-1}), C is the Cu^{2+} concentration after adsorption (mg·L^{-1}), V is the Cu^{2+} solution volume (L), and m is the mass of the absorbent (g).

Desorption study

The exhausted or spent adsorbent (Cu^{2+} loaded XWS) was obtained for the adsorption of 50 mg L^{-1} Cu^{2+} at pH 4. Then, Cu^{2+} loaded XWS was washed with distilled water to removal any unabsorbed Cu^{2+} and was dried at 353 K. The exhausted adsorbent was regenerated by 0.1 mol·L^{-1} HCl solution.

Column adsorption

Adsorption test in a fixed-bed column was carried out in one glass column (1 cm ID and 25 cm height), packed with 0.90 g XWS (height 5.4 cm). Solution with 40.0 mg L^{-1} Cu^{2+} was pumped in down flow mode at flow rate 9.9 mL·min^{-1} using a peristaltic pump. Samples from column effluent were collected at regular intervals to detect concentration of Cu^{2+}. Then breakthrough curve ($C_t/C_0 \sim t$) can be obtained.

RESULTS AND DISCUSSION

Characterization of materials

The pH of point zero charge of materials is helpful to confirm the surface charge at various solution pH values. The results of measurement of pH of point zero charge (pHpzc) for WS and XWS are shown in Figure 1. It was observed that pHpzc was 7.7 for WS and 8.8 for XWS. There is positive charge on the surface of material at solution pH lower than pHpzc, while there is negative charge at the solution pH above this value. The improvement of pHpzc after xanthan acidification indicates that the surface properties were changed.

The percentages of common elements are acquired by elemental analysis and the results are listed in Table 1. There is only sulfur (4.81%) for XWS, respectively. Compared with WS, the increased percentages of N and S were from CS_2 and EDA modification.

The X-ray diffraction (XRD) patterns of WS, ECH-WS, EDA-WS and XWS are presented in Figure. 2, suggesting that WS has two diffraction peaks around 16.5° and 22°, respectively, which are generated by the low crystallinity polysaccharide structure and the high crystallinity of cellulose. The diffraction patterns of ECH-WS and EDA-WS are basically the same. There is a strong diffraction peak near 20.3°, and the diffraction peak at 20.3° is also generated by the high crystallization of cellulose. The diffraction peaks

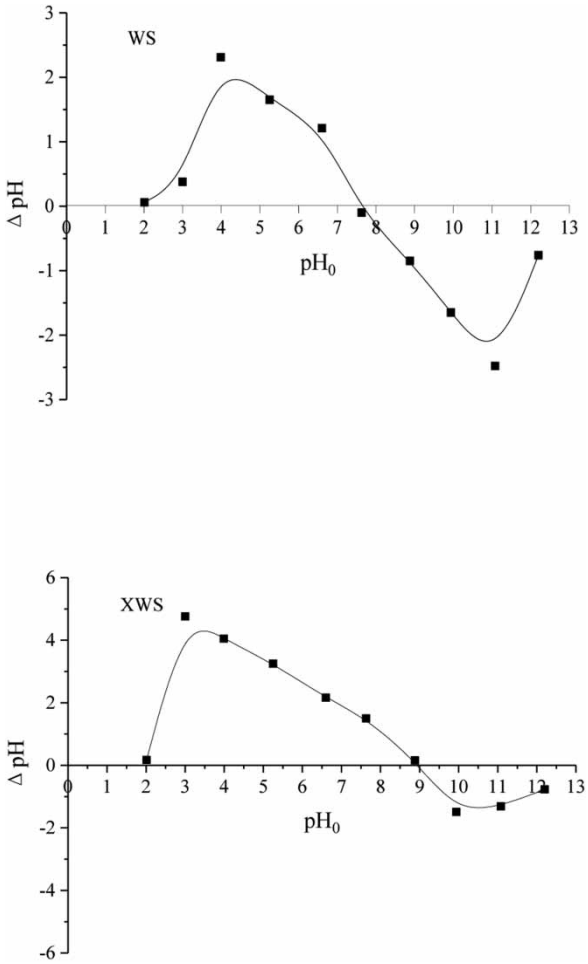

Figure 1 | Determination of pHpzc about WS and XWS.

Table 1 | Elemental analysis of four kinds of wheat straw (%) and comparison of adsorption quantity

Sample	N	C	H	S	q_e (mg·g^{-1})
WS	0.00	1.19	38.37	0.00	3.11
ECH-WS	0.00	45.41	6.50	0.00	12.0
EDA-WS	1.60	43.42	6.53	0.00	18.5
XWS	1.19	38.37	5.65	4.81	44.4

of XWS near 20.63° and 30.9° were also generated by the high crystallization of cellulose (Sánchez *et al.* 2016). By comparing the intensity of diffraction peaks of these three kinds of WS, it can be concluded that the intensity of diffraction peaks of the modified WS is in all cases smaller than that of WS, which also indicates that the crystal structure of the modified WS is destroyed and the order of crystal structure is reduced.

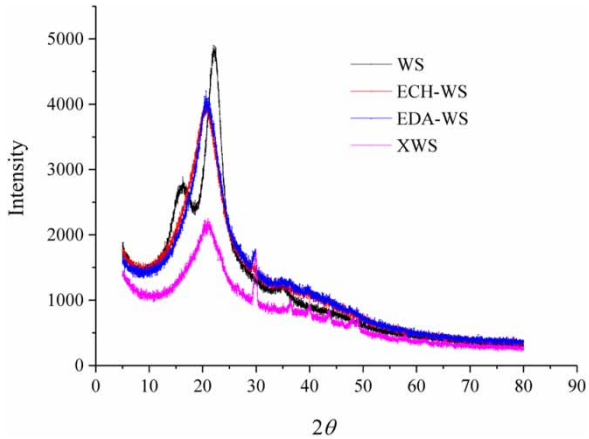

Figure 2 | XRD patterns of four wheat straws.

The FTIR analysis can offer some information about functional groups on the surface of materials (Chu *et al.* 2020). FTIR spectra of WS and XWS are presented in Figure 3. There is cellulose, lignin, etc. in plant materials. It is obviously seen from Figure 1 that FTIR analysis of WS and XWS displayed a number of absorption peaks, reflecting the complexity of the materials. There were −OH (peak at 3,416 cm^{-1}), carbonyl group (peak at 1,735 cm^{-1}), C – O – C (peak at 1,061 cm^{-1}), $-CH_2$ (peak at 1,061 cm^{-1}) etc. on the WS surface from FTIR analysis (Han *et al.* 2010). For XWS, the peak at 1,735 cm^{-1} was not observed, as ethylenediamine can react with carbonyl groups. A new peak for XWS at 2,065 cm^{-1} was formed by the stretching vibration of −SH, which also indicated that −SH was successfully introduced into the surface of WS; that is, sulfur modified WS was successfully obtained. After modification, the structure of WS is relatively stable.

Adsorption study in batch mode

Effect of contact time on adsorption quantity

Reactive time is often of concern during adsorption study. The effect of contact time is depicted in Figure 4. It was clearly noticed from Figure 4 that values of q_t increased significantly at the initial stage, and then increased slowly until reaching the adsorption equilibrium after 250 min. In the initial phase, the surface sites were available for adsorption, then the adsorption of Cu^{2+} was in a gradual adsorption phase, and finally the Cu^{2+} uptake reached equilibrium (q_e to 44.4 mg·g^{-1}). In the next study, contact time is 300 min in order to reach adsorption equilibrium.

Under the same conditions, q_e values for WS, ECH-WS and EDA-WS are also listed in Table 1. It was shown from

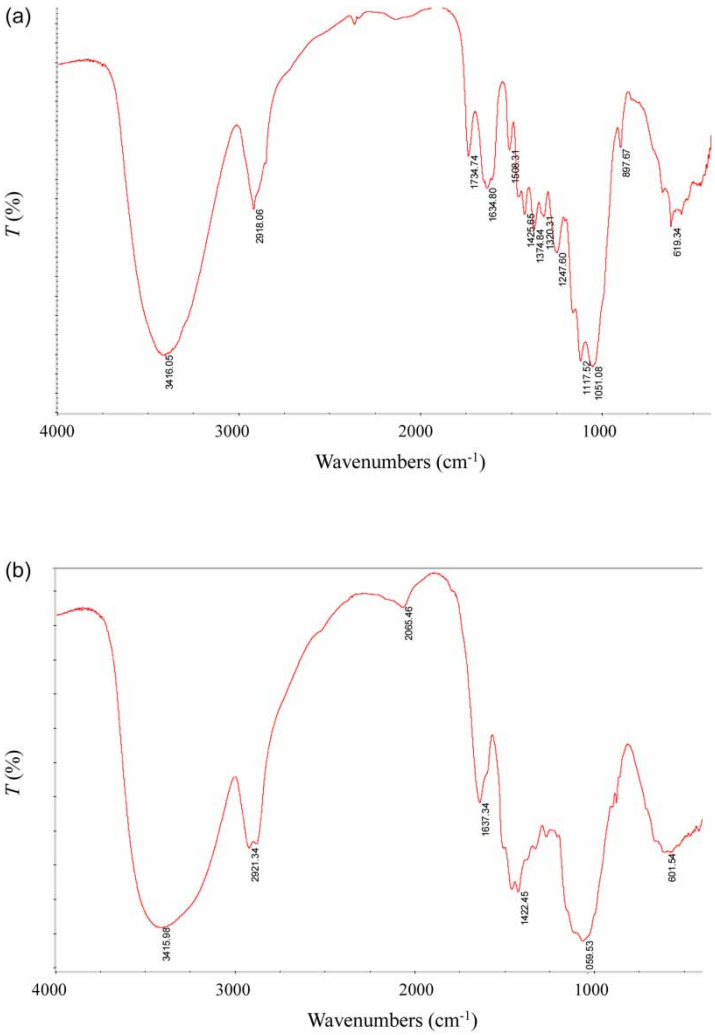

Figure 3 | FTIR of WS (a) and XWS (b).

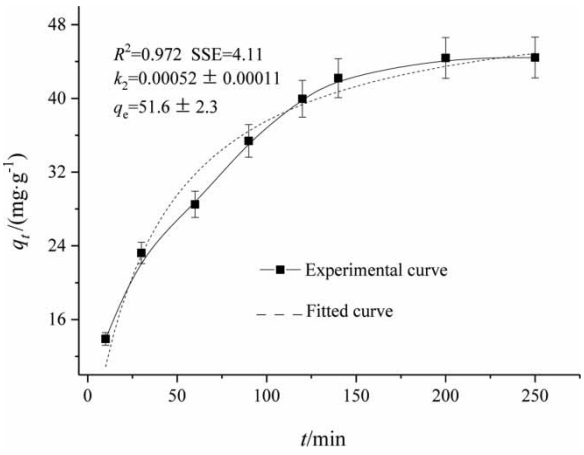

Figure 4 | Effect of contact time on adsorption quantity and the fitted results.

Table 1 that there was highest adsorption capability about XWS for removal of Cu^{2+}. This is due to xanthate existing in the surface, which has good adsorption capacity toward some cationic metal ions.

The pseudo-second-order kinetic model was applied to fit kinetic data. The expression is as follows (Ho *et al.* 2011):

$$q_t = \frac{k_2 q_e^2 t}{1 + k_2 q_e t} \quad (2)$$

where q_t is adsorption quantity (mg·g^{-1}) at time (t); q_e is adsorption quantity at equilibrium (mg·g^{-1}); k_2 (mg·g^{-1}·min^{-1}) is kinetic rate constant.

Nonlinear regression method was selected to fit the kinetic results, and the obtained results are shown in Figure 4.

It was noticed from Figure 4 that there were higher determined coefficient (R^2) and lower values of SSE, and the value of q_e from this model was not far from the value of q_e from experiment. ($SSE = \Sigma(q-q_c)^2$, where q and q_c are the experimental value and calculated value from model, respectively.) Furthermore, the fitted curve was also not far from the experimental curve. So it can be concluded that the pseudo-second-order kinetic model can be used to predict the kinetic process of Cu^{2+} adsorption onto XWS.

Effect of common salts on adsorption

There are common salts in metal ion wastewater, so it is necessary to study the behavior of coexisting salt in solution on adsorption process. The results are presented in Figure 5.

It was observed from Figure 5 that the values of q_e increased slightly with the increase in the NaCl concentration, and then adsorption quantity showed no change even with further large salt concentration. So it is implied that the major mechanism is the coordinate action between copper ion and xanthate and there is no interaction force between Na^+ and the adsorbent. This is significant regarding no effect of salt on adsorption quantity, and it was inferred that XWS can be applied to bind Cu^{2+} in real wastewater. It is concluded that complexation, not ionic exchange or electrostatic attraction, is the main mechanism of Cu^{2+} binding. Based on the fact that the sewage contains other metal ions, NaCl concentration was maintained at 0.02 mol·L^{-1} in the following experiments.

Effect of solution pH on adsorption

Solution pH is also an important parameter in adsorption process, as pH can affect the protonation and deprotonation of the surface of the adsorbate and adsorbent. When the pH value of the solution is less than or equal to 6, copper ions exist mainly in the form of Cu^{2+} in the solution. Figure 6 shows the effect of solution pH on Cu^{2+} adsorption quantity by XWS. Under the condition of strong acidity, the unit adsorption capacity of XWS is relatively small. When pH value increased from 2.0 to 3.0, adsorption capacity increased significantly (from 8.44 mg·g^{-1} to 26.9 mg·g^{-1}). At pH = 5.0, value of q_e was 47.5 mg·g^{-1}. Although the increase of pH value is conducive to adsorption, metal ions are easy to precipitate at pH over 6. The adsorption of positive metal ions is not favored at lower pH of solution.

Adsorption isotherm curve

Some useful information can be clearly obtained from adsorption isotherm curve. The experimental results are depicted in Figure 7. It was noticed that the values of q_e for Cu^{2+} adsorption sharply increased with the increase of Cu^{2+} concentration, then increased more slowly and reached near equilibrium (57.5 mg·g^{-1}). This may be attributed to the concentration gradient being the driving force for the adsorption of Cu^{2+} on the XWS.

Adsorption isotherm models are often considered to fit the equilibrium results, and Langmuir model is used to fit the results. The expression is as follows (Liu & Liu 2008; Han *et al.* 2010):

$$q_e = \frac{q_m K_L c_e}{1 + K_L c_e} \tag{3}$$

where q_m is the maximum adsorption capacity (mg·g^{-1}) and K_L is a constant related to the affinity of the binding sites and energy of adsorption (L·mg^{-1}).

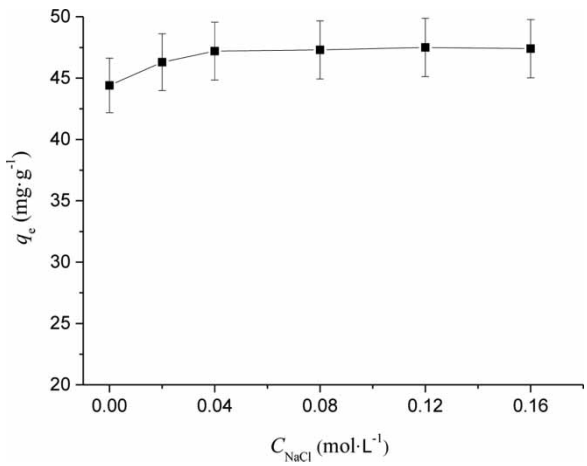

Figure 5 | Effect of NaCl concentration on adsorption.

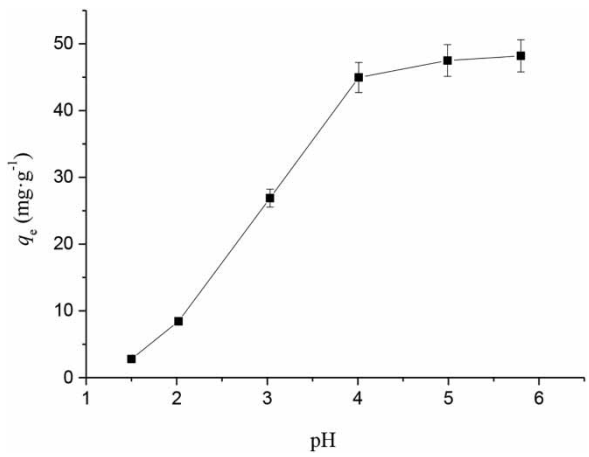

Figure 6 | Effect of solution pH on adsorption.

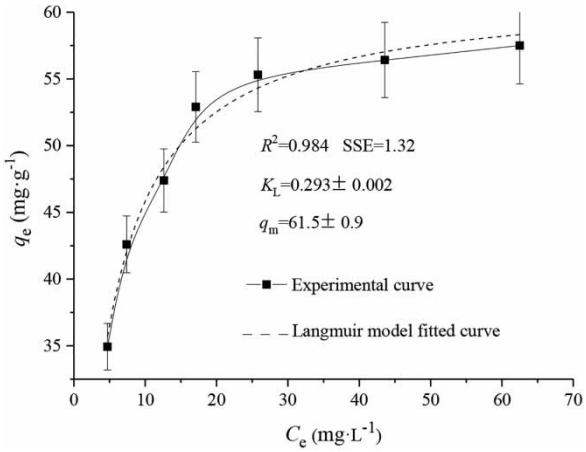

Figure 7 | Adsorption isotherm curve of Cu^{2+} adsorption at 303 K.

The Langmuir model is used to fit the equilibrium data using nonlinear regression analysis, and the results are also shown in Figure 7.

It was obviously seen from Figure 7 that the value of R^2 was over 0.98, and the error was relatively small; the value of q_m was also close to the experimental result. This implied that Cu^{2+} adsorption onto XWS is dominated by monolayer adsorption and this model can describe the equilibrium process and predict the adsorption capacity.

Effect of temperature on adsorption quantity and thermodynamic analysis of adsorption

At $C_0 = 50$ mg·L^{-1}, the values of q_e were 37.5, 44.4, 46.2 mg·g^{-1} g at 293, 303 and 313 K, respectively. This showed that the process is endothermic and it is in favor of Cu^{2+} adsorption at higher temperature.

Thermodynamic studies reveal the mechanism of the reaction. Thermodynamic parameters such as enthalpy change (ΔH, kJ·mol^{-1}), Gibbs free energy change (ΔG, kJ·mol^{-1}) and entropy change (ΔS, J·mol^{-1}·K^{-1}) are defined using the following equations:

$$K_c = C_{ad,e}/C_e \quad (4)$$

$$\Delta G = -RT \ln K_c \quad (5)$$

$$\Delta G = \Delta H - T\Delta S \quad (6)$$

where C_{ad} is the concentration of Cu^{2+} on the XWS at equilibrium (mg·L^{-1}), C_e is the concentration of Cu^{2+} in the solution at equilibrium (mg·L^{-1}), K_c is apparent adsorption equilibrium constant, R is the universal gas constant (8.314 J·mol^{-1}·K^{-1}), T is the solution temperature (K).

The thermodynamic data of the adsorption of Cu^{2+} by XWS were obtained by using the thermodynamic formula, as shown in Table 2. According to Table 2, values of parameters ($\Delta S < 0$, $\Delta H > 0$, $\Delta G < 0$) showed that Cu^{2+} adsorption onto XWS was a spontaneous and endothermic, entropy reduction process. At the same time, value of ΔH value is around 40 kJ·mol^{-1}; adsorption is mainly a coordination effect. So the process of adsorption is mainly coordination.

Desorption study

Desorption study is not only in favor of explaining the mechanism of adsorption, but also making the process more economical and maybe recovering valuable compounds (Su *et al.* 2013; Zhao *et al.* 2017; Liu *et al.* 2020). The results are 55% of desorption efficiency using 0.1 mol·L^{-1} HCl solution. This showed that the reaction between Cu^{2+} and xanthate onto XWS was strong and not easily desorbed.

Adsorption in column mode

The property of Cu^{2+} adsorption onto XWS can be further carried out by column mode, as this performance is continuous. The breakthrough curve of Cu^{2+} adsorbed onto XWS is illustrated in Figure 8. It was markedly seen that the shape of curve was 'S' type. The values of $t_{0.05}$ (breakthrough time) and $t_{0.5}$ (half breakthrough time) (at time of $C_t/C_0 = 0.5$) were 46 min, respectively.

The adsorption uptake from breakthrough curve ($q_{e(exp)}$) was obtained using following expression:

$$q_{e(exp)} = \frac{vA}{1000m} = \frac{v}{1000m}\int_{t=0}^{t=t_{total}} (C_0 - C_t)dt \quad (7)$$

where v, t_{total} and A are volumetric flow rate (mL·min^{-1}), total flow time (min), and the area under the breakthrough curve, respectively; m is the dry weight of XWS (g).

According to Equation (7), the value of $q_{e(exp)}$ was 27.5 mg·g^{-1}.

Table 2 | Thermodynamic parameters of Cu^{2+} adsorption onto XWS

		ΔG (kJ·mol^{-1})		
ΔH (kJ·mol^{-1})	ΔS (J·mol^{-1}·K^{-1})	293 K	303 K	313 K
40.3	−157	−5.61	−7.29	−8.74

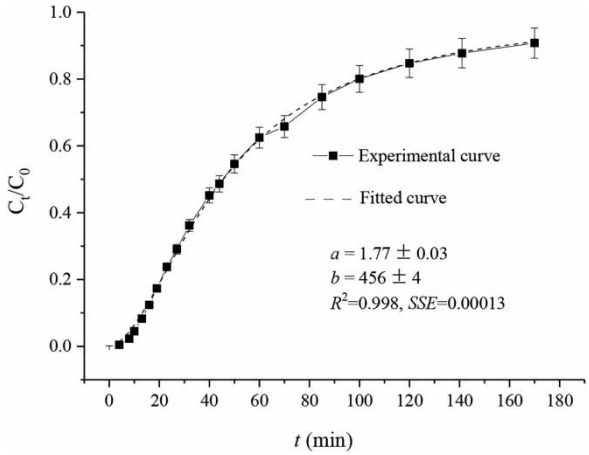

Figure 8 | Breakthrough curve and fitted curve of Cu^{2+} adsorption on XWS (XWS m = 0.90 g, h = 5.4 cm, C_0 = 40 mg·L^{-1}, v = 10 mL·min^{-1}).

The length of the mass transfer zone (L) was calculated as the following expression (Yamil *et al.* 2020):

$$L = h\left(1 - \frac{t_b}{t_e}\right) \tag{8}$$

where h is the height of the fixed bed (cm), breakthrough time (t_b) and exhaustion time (t_e) were obtained from this curve, considering $C_t/C_0 = 5\%$ and $C_t/C_0 = 95\%$, respectively (Georgin *et al.* 2019).

So value of L was 5.1 cm through calculation, and this was a relatively short length.

Yan model is selected to fit the experimental results. The expression is as follows (Yan *et al.* 2001; Song *et al.* 2011; Dotto & McKay 2020; Li *et al.* 2020):

$$\frac{C_t}{C_0} = 1 - \frac{1}{1 + (vt/b)^a} \tag{9}$$

where both a and b are parameters of this model.

Using nonlinear regressive analysis method, the values of a, b, determined coefficient (R^2), SSE and fitted curve are also shown in Figure 8. There was a higher value of R^2 and lower value of SSE, while the value of q_0 (bC_0/m) from Yan model was 20.3 mg·g^{-1}, smaller than $q_{e(exp)}$. Moreover, the fitted curve shown in Figure 8 is very close to the experimental curve. It was implied that Yan model can predict the column process.

CONCLUSION

XWS for the removal of Cu^{2+} from solution has been successfully prepared though chemical reaction, exhibiting good adsorption capacity. The coexisting common salts were slightly advantageous for Cu^{2+} adsorption. The effects of column height, flow rate and initial concentration on the adsorption process were studied in dynamic experiments. By investigating the isotherms and kinetics fitting data, it was indicated that Langmuir model and pseudo-second-order kinetic model were suitable to fit the equilibrium data and kinetic data, respectively. The adsorption mechanism of Cu^{2+} onto XWS is mainly coordination. Yan model could well describe the column curve. So XWS has potential with good adsorption property for removal of Cu^{2+} from solution.

ACKNOWLEDGEMENTS

This work was financially supported by the Henan province basis and advancing technology research project (142300410224).

DATA AVAILABILITY STATEMENT

All relevant data are included in the paper or its Supplementary Information.

REFERENCES

Bhatnagar, A. & Sillanpaa, M. 2010 Utilization of agro-industrial and municipal waste materials as potential adsorbents for water treatment – a review. *Chem. Eng. J.* **157** (2–3), 277–296.

Chauhan, D. & Sankararamkrishnan, N. 2008 Highly enhanced adsorption for decontamination of lead ions from battery wastewaters using chitosan functionalized with xanthate. *Bioresour. Technol.* **99**, 9021–9024.

Chu, D. Y., Ye, Z. L. & Chen &, S. H. 2020 Interactions among low-molecular-weight organics, heavy metals, and Fe(III) during coagulation of landfill leachate nanofiltration concentrate. *Waste Manage.* **104**, 51–59.

Deng, S. B. & Ting, Y. P. 2005 Characterization of PEI-modified biomass and biosorption of Cu(II), Pb(II) and Ni(II). *Water Res.* **39**, 2167–2177.

Dong, J. J., Du, Y. Y., Duyu, R. S., Shang, Y., Zhang, S. S. & Han, R. P. 2019 Adsorption of copper ion from solution by polyethylenemine modified wheat straw. *Bioresour. Technol. Rep.* **6**, 96–102.

Dotto, G. L. & McKay, G. 2020 Current scenario and challenges in adsorption for water treatment. *J. Environ. Chem. Eng.* **8**, 103988.

Fu, F. L. & Wang, Q. 2011 Removal of heavy metal ions from wastewaters: a review. *J. Environ. Manage.* **92**, 407–418.

Georgin, J., Franco, D., Drumm, F. C., Grassi, P. A., Netto, M. S., Allasia, D. & Dotto, G. L. 2019 Powdered biosorbent from the mandacaru cactus (*Cereus jamacaru*) for discontinuous and continuous removal of Basic Fuchsin from aqueous solutions. *Powder Technol.* **364**, 584–592.

Gorgievski, M., Bozic, D., Stankovic, V., Strbac, N. & Serbula, M. 2013 Kinetics, equilibrium and mechanism of Cu^{2+}, Ni^{2+} and Zn^{2+} ions biosorption using wheat straw. *Ecol. Eng.* **58**, 113–122.

Han, R. P., Zhang, L. J., Song, C., Zhang, M. M., Zhu, H. M. & Zhang, L. J. 2010 Characterization of modified wheat straw, kinetic and equilibrium study about copper ion and methylene blue adsorption in batch mode. *Carbohyd. Polym.* **79**, 1140–1149.

Hashim, M. A., Mukhopadhyay, S., Sahu, J. N. & Sengupta, B. 2011 Remediation technologies for heavy metal contaminated groundwater. *J. Environ. Manage.* **92**, 2355–2388.

Ho, Y. S., Ng, J. C. Y. & McKay, G. 2011 Kinetics of pollutant sorption by biosorbents: review. *Sep. Purif. Method.* **29**, 189–232.

Li, J. Y., Ma, J., Guo, Q. H., Zhang, S. L., Han, H. Y., Zhang, S. S. & Han, R. P. 2020 Adsorption of hexavalent chromium from solution using modified walnut shell. *Water Sci. Technol.* **81**, 824–833.

Liang, S., Guo, X. Y., Feng, N. C. & Tian, Q. H. 2009 Application of orange peel xanthate for the adsorption of Pb^{2+} from aqueous solutions. *J. Hazard. Mater.* **170**, 425–429.

Liu, Y. & Liu, Y. J. 2008 Biosorption isotherms, kinetics and thermodynamics. *Separ. Purif. Technol.* **61**, 229–242.

Liu, M. Y., Zhang, X. T., Li, Z. H., Qu, L. B. & Han, R. P. 2020 Fabrication of zirconium (IV)-loaded chitosan/Fe_3O_4/graphene oxide for efficient removal of alizarin red from aqueous solution. *Carbohyd. Polym.* **248**, 116792.

Sánchez, R., Espinosa, E., Domínguez-Robles, J., Loaiza, J. M. & Rodríguez, A. 2016 Isolation and characterization of lignocellulose nanofibers from different wheat straw pulps. *Int. J. Biol. Macromol.* **92**, 1025–1033.

Shang, Y., Zhang, J. H., Wang, X., Zhang, R. D., Xiao, W., Zhang, S. S. & Han, R. P. 2016 Use of polyethylenemine modified wheat straw for adsorption of Congo red from solution in batch mode. *Desalin. Water Treat.* **57**, 8872–8883.

Song, J. Y., Zou, W. H., Bian, Y. Y., Su, F. Y. & Han, R. P. 2011 Adsorption characteristics of methylene blue by peanut husk in batch and column mode. *Desalination* **265**, 119–125.

Su, Y. Y., Zhao, B. L., Xiao, W. & Han, R. P. 2013 Adsorption behavior of light green anionic dye using cationic surfactant modified wheat straw in batch and column mode. *Environ. Sci. Pollut. Res.* **20**, 5558–5568.

Wang, Z. W., Han, P., Jiao, Y. B., He, X. T., Dou, C. C. & Han, R. P. 2011 Adsorption of Congo red using ethylenediamine modified wheat straw. *Desalin. Water Treat.* **30**, 195–206.

Xu, X., Gao, Y., Gao, B. Y., Tan, X., Zhao, Y. Q., Yue, Q. Y. & Wang, Y. 2011 Characteristics of diethylenetriamine-crosslinked cotton stalk/wheat stalk and their biosorption capacities for phosphate. *J. Hazard. Mater.* **192**, 1690–1696.

Yamil, L. d. O. S., Jordana, G., Dison, S. P., Franco, M. S., Netto, P. G., Daniel, G. A., Piccilli, M. L. S. & Oliveira, G. L. D. 2020 Powdered biosorbent from pecan pericarp (*Carya illinoensis*) as an efficient material to uptake methyl violet 2B from effluents in batch and column operations. *Adv. Powder Technol.* **31**, 2843–2852.

Yan, G., Viraraghavan, T. & Chen, M. A. 2001 New model for heavy metal removal in a biosorption column. *Adsorpt. Sci. Technol.* **19**, 25–43.

Yu, Z. S., Han, H. W., Feng, P. Y., Zhao, S., Zhou, T. Y., Kakade, A., Kulshrestha, S., Majeed, S. & Li, X. K. 2020 Recent advances in the recovery of metals from waste through biological processes. *Bioresour. Technol.* **297**, 122416.

Zhang, R. D., Zhang, J. H., Zhang, X. N., Dou, C. C. & Han, R. P. 2014 Adsorption of Congo red from aqueous solutions using cationic surfactant modified wheat straw in batch mode: kinetic and equilibrium study. *J. Taiwan Inst. Chem. E.* **45**, 2578–2583.

Zhao, B. L., Xiao, W., Shang, Y., Zhu, H. M. & Han, R. P. 2017 Adsorption of light green anionic dye using cationic surfactant-modified peanut husk in batch mode. *Arab. J. Chem.* **10** (s2), 3595–3602.

Zhong, Q. Q., Yue, Q. Y., Li, Q., Gao, B. Y. & Xu, X. 2014 Removal of Cu(II) and Cr(VI) from wastewater by an amphoteric sorbent based on cellulose-rich biomass. *Carbohyd. Polym.* **111**, 788–796.

Zhou, T. B., Lu, J., Zhou, Y. & Liu, Y. D. 2019 Recent advances for dyes removal using novel adsorbents: a review. *Environ. Pollut.* **252**, 352–365.

First received 12 June 2020; accepted in revised form 26 September 2020. Available online 7 October 2020